ICAS 2020 International Council of the Aeronautical Sciences SHANGHAI
32nd Congress of the International Council of the Aeronautical Sciences
September 6-10, 2021
Pudong Shangri-La, Shanghai, China

Numerical Study of High Temperature Transverse Pulse Jet in the Supersonic Combustion Chamber

Wang Yuhan[1], Qian guangping[2]
[1]Shanghai Aircraft Design and Research Institute, 5188 Jing Ke Road, Shanghai, 201210, China.
wangyuhan1@comac.cc
[2]Shanghai Aircraft Design and Research Institute, 5188 Jing Ke Road, Shanghai, 201210, China.
qianguangping@comac.cc

Abstract

In order to increase the fuel combusted efficiency, the numerical simulation of supersonic combustion flow field with high temperature transverse pulse hydrogen jet in the scramjet combustion chamber is carried out. The combustion flow fields are calculated with Reynold-averaged multi-component N-S equations, based on the finite volume method. The result shows with the same injection parameters as steady injection scheme, the pulse injection scheme has a positive effect on the lateral diffusion of hydrogen and water in the pulse interference zone; The maximum of amount of hydrogen combusted could reach 25.46% in the pulse interference zone, the total pressure recovery coefficient is 1.4% greater at the exit section of combustion chamber, and the inner thrust is 9.0% increased.

Keywords: High temperature jet, numerical simulation, supersonic combustion, transverse pulse injection

1. Introduction

In order to improve the efficiency of fuel and air mixing and combustion as much as possible in the scramjet combustion chamber with limited time and space, the spatial layout of jet and the injection parameters are always the general ways to think about [1]-[4]. As it becomes widely used, the time effect of fuel injection is being taken seriously. Williams [5] explored the influence of sinusoidal pulse jet on jet penetration depth at different frequencies by using Fluent. The results showed that the 16kHz pulse jet achieved the best improvement of jet penetration depth in both nearby and faraway fields of jet. Cutler and his team [6] studied the mixing characteristics of pulsed helium jet in supersonic tube flow. It was concluded that the cross-section plume size decreased with the increase of helium penetration depth. Kouchi [7] found that the penetration depth of pulse jet could be adjusted by changing the pulse period under the condition of fixed mass flow rate of nitrogen injection. ZHOU Song-bai [8] used the pulse injection scheme on the NAL dual-mode ramjet engine model. It was initially obtained that the pulse jet could reduce the separation in the isolator, the fuel enters the combustion chamber in a “pellet” way, and the combustion surface is shorter in the axial direction. It’s worthy to make a further study on the effect of pulse injection scheme on the fuel mixing and combustion characteristics.

In this paper, the combustion flow field with the steady injection scheme and pulse injection scheme are numerically simulated. When the jet is open, the injection parameters are the same as the steady injection scheme, which means the mass flux of hydrogen is only the half of steady injection in the characteristic time. The flow field characteristics, distributions of hydrogen and water, amount of hydrogen combusted, total pressure recovery coefficient and inner thrust of two different fuel injection schemes are compared.

2. Geometry and Methodology

2.1 Numerical simulation method

In this paper, the finite volume scheme is used to solve Reynold-Averaged two-dimensional multi-component N-S equations based on Hybrid Grid Technology. The second-order Roe scheme and SST k-ω two-equation are employed for spatial discretization and turbulence model. Dual time-stepping for implicit scheme is adopted, and five-stage Runge-Kutta scheme is used for the sub-iteration. The combustion reaction model is the 7 component 8 reaction hydrogen-air combustion model proposed by Moretti. The specific solution method has been described in references [9]-[11].

2.2 Calculation Model

The model used is a 2D scramjet combustor with backward-facing step, and the detailed measurements are shown in Figure 1, in which the X and Y direction respectively represents the axial and transverse direction. The jet is 2.5mm wide and the backwards-stepping is 5mm height. Five pressure monitoring points are set during the unsteady calculation. The coordinates are shown in Table 1, and the positions are marked with numbers 1 to 5 in Figure 1.

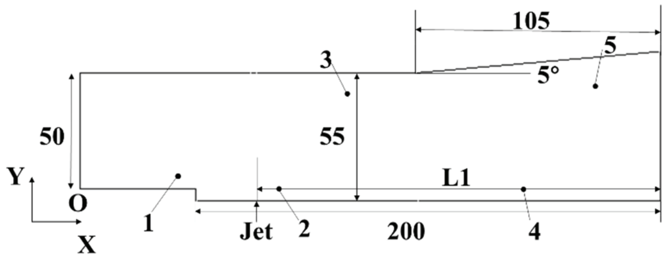

Figure 1 – Schematic of scramjet combustor (unit: mm).

Table 1 – Coordinates of the monitoring points

Point	X/mm	Y/mm
1	46	5
2	86.6	0
3	120	40
4	209	0
5	222	42.2

2.3 Mesh Independence Verification

To study the effect of high temperature transverse pulse injection on the supersonic combustion flow field, the computational conditions are listed in Table 2. P_∞, Ma_∞ and T_∞ indicate the static pressure, Mach number, and static temperature of the inflow respectively, while the P_j, Ma_j and T_j describe the injection parameters when the jet is open. Three mesh distributions are calculated to ensure that the mesh quantity is independent with the numerical results. The detailed information about meshed are shown in Table 3, in which Nc and h_1 identify the number of mesh cells and the height of first layer mesh from the surface. The distributions of the pressure coefficient and the mass fraction of the combustion product water (Y_H_2O) on the characteristic line (Y=4mm) are used to verify the mesh independence, shown as Figure 2. Since the lines of M2 and M3, denoting pressure coefficient and mass fraction of water, basically coincide, M2 is fine enough for the later calculation. The mesh of whole calculated domain and near the backward-facing step and jet are shown in Figure 3.

Table 2 – Computational Conditions

Free Stream Conditions			Jet Flow Conditions		
p_∞/kPa	Ma_∞	T_∞/K	p_j/MPa	Ma_j	T_j/K
50.66	2.5	1000	0.15	1.0	300

Table 3 – Meshes used to verify the mesh independence

Name	*Nc*	*y+*	h_1/m
M 1	52000	1.2	3.8 e-6
M 2	99000	1.0	3.2 e-6

M 3	142000	0.8	2.5 e-6

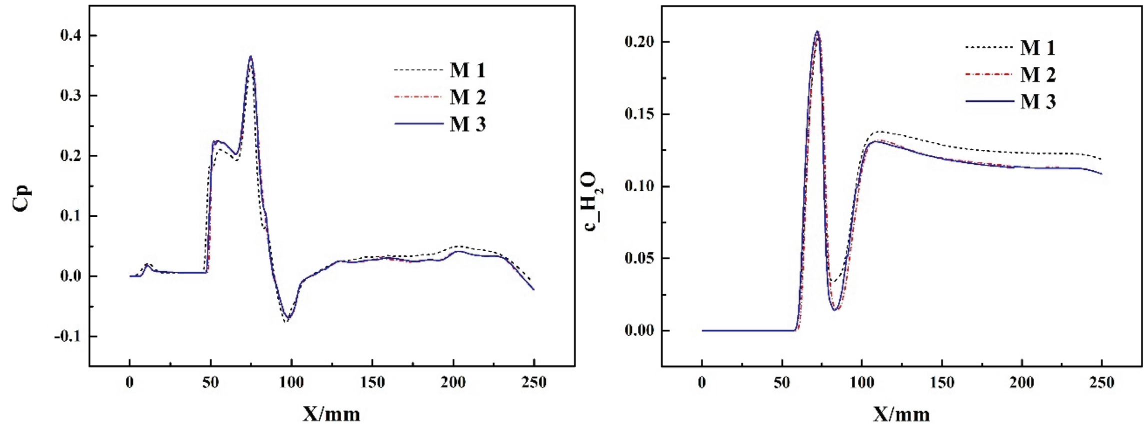

Figure 2 – Typical parameters distribution along the characteristic line

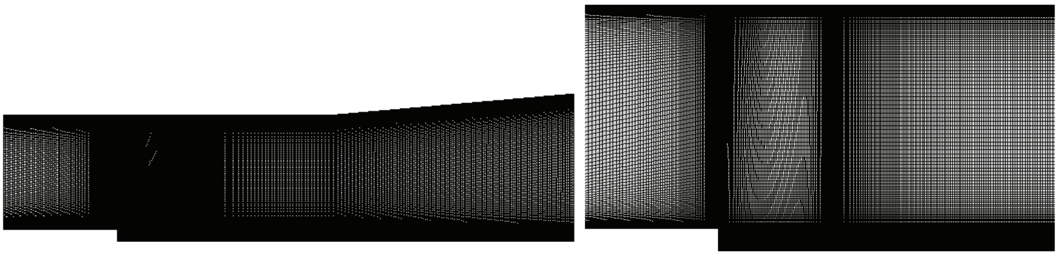

Figure 3 – Computational mesh

3. Results and Discussions

3.1 Pulse Parameters Analysis

The time parameters calculation methods of pulse jet time parameter and combustion flow field characteristic parameter are given below. Pulse injection starts after the stable transverse hydrogen injection combustion flow field established, where the time is defined as 0. The pulse injection scheme is shown in Figure 4, taking hydrogen transverse injection speed V_j as an example. The period of hydrogen ejected from the jet to the exit of combustor can be gotten according to (1) [8].

$$t_1 = \frac{L_1}{V_\infty} = \frac{L_1}{Ma_\infty \cdot \sqrt{\gamma_\infty R_\infty T_\infty}} \tag{1}$$

L_1 is the distance from the center line of the jet to the exit of combustor (marked in Figure 1), V_∞, γ_∞ and R_∞ respectively represents inflow velocity, specific heat ratio and gas constant. In this paper, t=0.2ms. According to the reference [8], this time period is divided into five pulse periods, so that each pulse period T equals 0.04ms, it is also called characteristic time. During the characteristic time, Δt_1 / Δt_2 = 0.5, so that $\Delta t_1 = \Delta t_2$ = 0.02ms.

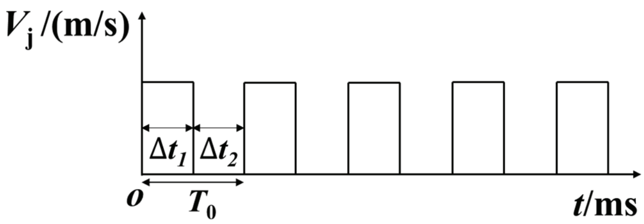

Figure 4 – Pulse injection scheme

In the pulse injection scheme, the mass flux of hydrogen ejected is zero when the jet is off, so that the normal combustion efficiency formula [12] is no longer applicable. Therefore, a new characteristic parameter, amount of hydrogen combusted ($Q(H_2)_{burn}$), is defined to describe the performance of combustion on the characteristic section.

$$Q(H_2)_{\text{burn}} = \int_A \frac{2}{18} \rho u \, \alpha_1 dA \tag{2}$$

ρ is density of the mixture, u is axial velocity of the mixture, and α_1 is mass fraction of water.

The total pressure recovery coefficient [13] is defined as the ratio of the mass weighted average of the total pressure on the characteristic section to the mass weighted average of the total import pressure on the inlet section.

$$\sigma = \frac{\dot{m}_0}{\int_{A(X=0)} p_t \rho u dA} \cdot \frac{\int_{A(X)} p_t \rho u dA}{\dot{m}(x)} \tag{3}$$

P_t, $\dot{m}(x)$ is total pressure and mass flux of the mixture on the characteristic section, respectively. $\dot{m}_0$ represents mass flux of inflow.

The inner thrust of combustion chamber [14] is defined below:

$$F_{int} = (P_e A_e + \dot{m}_e u_e) - (P_0 A_0 + \dot{m}_0 u_0) \tag{4}$$

With the subscript e means the parameters of exit of the combustor, and the subscript 0 stands for the inlet parameters. A is the area of section, and u is the velocity of mixture flow.

3.2 Flow Field Characteristics

The pressure of monitoring points changes with time are shown in Figure 5. The stable-pulse-flow-field establishment needs 1.5ms.

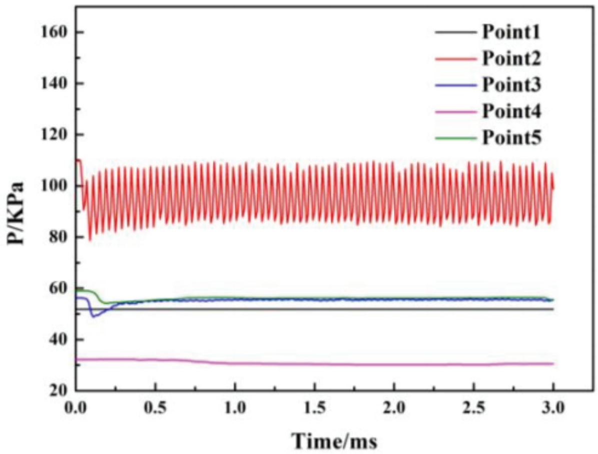

Figure 5 – Pressure variations over time of five monitoring points under non-reacting flow

The combustion flow fields of steady injection and pulse injection are given in Figure 6. The steady injection flow filed tells the complicated shock structures: The backward-stepping shock forms when supersonic inflow passing the corner of backward-stepping. Because of the interaction between inflow and jet, the bow shock appears in front of the jet. The two shocks are fused, forming one shock, and reflected on the upper wall. The upper wall separation shock forms as the boundary layer separated. Behind of the separated area, the upper wall reattachment shock shows up. The boundary layer behind the jet is separated and reattached, forming the jet reattachment shock. When the pulse flow filed stably established, the reflection point of backward- stepping shock at the upper wall moves behind, because of the weakened interaction between jet and inflow. The bow shock forms periodically, the jet reattachment shock cyclically moves left and right. The effects of pulse interference on the flow field is only concentrated in the local region, marked with the dash line, which means pulse injection will not bring excessive load to the combustion chamber. The pulse interference changes periodically, which is consistent with the pulse period.

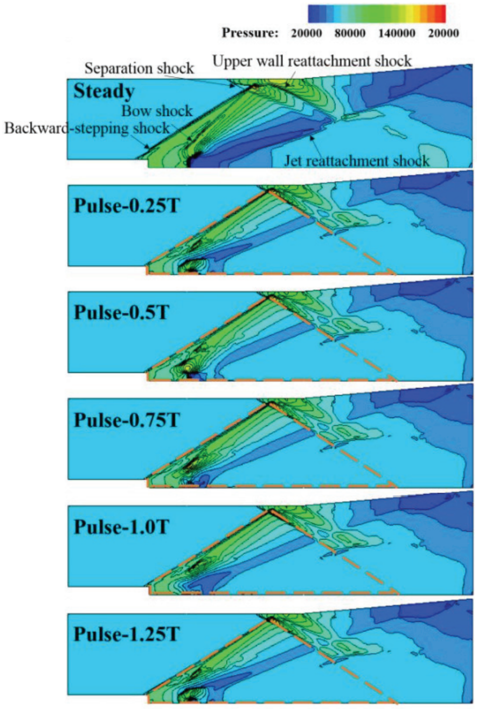

Figure 6 – Pressure contour lines of reacting flow field

The mass fraction of hydrogen is shown in Figure 7. When the injection is steady, hydrogen accumulates around the jet, completely blocking the mainstream air, so that the main mixing happens downstream. After the stable pulse flow field built, mainstream enters with the switch of jet, making the mix starts from the jet. The hydrogen penetration depth is smaller than the steady because of the half mass flux ejected, leading to a weaker interference of jet and inflow. Fig. 8 gives the transverse distribution of hydrogen mass fraction over the section of X=110mm, which is within the area of pulse interference. When the pulse injection adopted, Y_H_2 is not decreased from 1, which means hydrogen and air have been mixed near the wall. The steady and pulse injection have basically the same hydrogen diffusion boundary, defined as the value of Y when Y_H_2 is equal to 0, since $Y(Y\_H_2=0)_{Steady}$=8.82mm, $Y(Y\_H_2=0)_{Pulse}$=8.89mm.

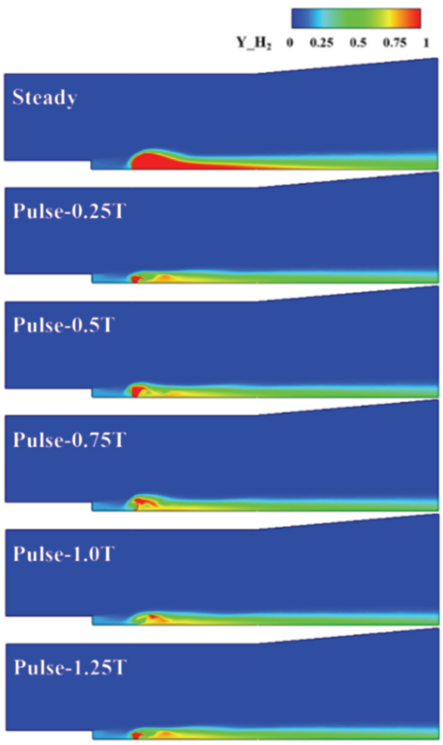

Figure 7 – Hydrogen mass fraction contours distribution

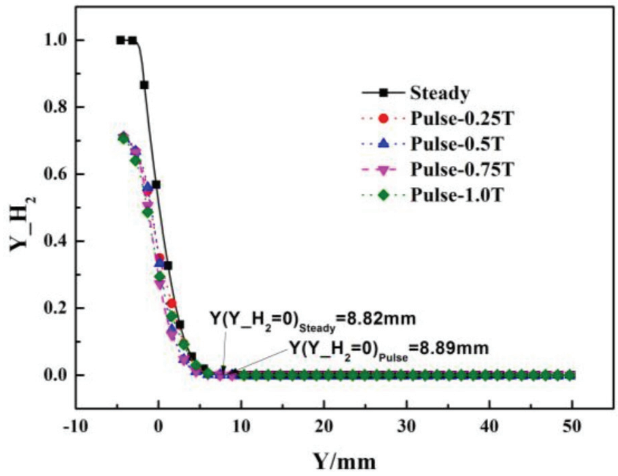

Figure 8 – Transverse distribution of hydrogen mass fraction on the section of X=110mm

Figure 9 shows the mass fraction distribution of water. The area around jet contains water, where is total without water in the steady injection scheme. Within the area of pulse interference, the distribution of water changes periodically. The transverse distribution of water mass fraction on the section of X=110mm is shown in Figure 10. Y_H_2O of the first point in pulse injection lines is bigger than zero, which indicates the distribution of water has been extended to the bottom wall. The maximum mass fraction of water is 0.195 in pulse injection and 0.181 in steady injection, which tells the pulse injection could promote the combustion. On the other hand, the water diffusion boundary of pulse injection scheme is a little higher than the steady.

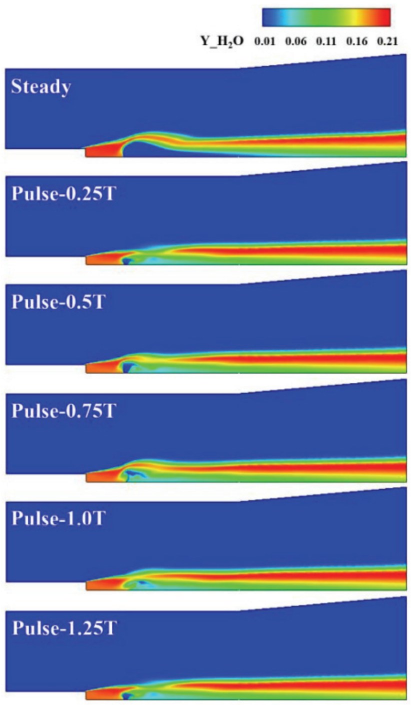

Figure 9 – Water mass fraction contours distribution

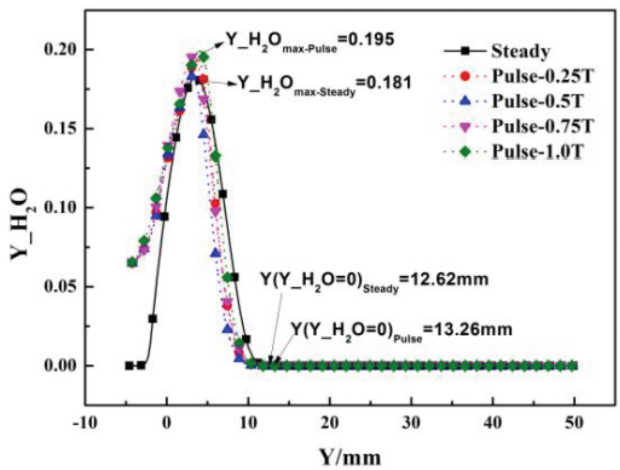

Figure 10 – Transverse distribution of water mass fraction on the section of X=110mm

Figure 11, Figure 12 and Table 4 have compared three parameters to discuss the performance in the combustion chamber. The amount of hydrogen combusted is shown in Figure 11. The pulse injection scheme, which saves half of fuel, could even more hydrogen combusted in the region around jet, where is the pulse interference zone. The maximum increase reaches 25.46%(X=127.5mm). However, when the region is far from pulse interference zone, the amount of hydrogen combusted is smaller than steady injection scheme since the decreased mass flux of hydrogen ejected becomes the main influence, and on the exit section of combustion chamber decreased about 10.12%. The total pressure recovery coefficient is given in Figure 12. On the exit section of chamber, the total pressure recovery coefficient is 0.8286 with pulse jet and 0.8174 with the steady jet, where is increased by 1.4%. Table 4 is the inner thrust comparison. adopting the pulse injection, the inner thrust is increased 9.0% only with a half fuel in the same time period.

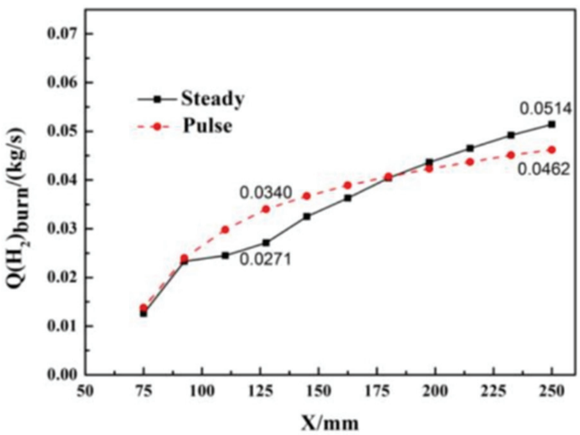

Figure 11 – Amount of Hydrogen combusted downstream of X=75mm along the axial direction

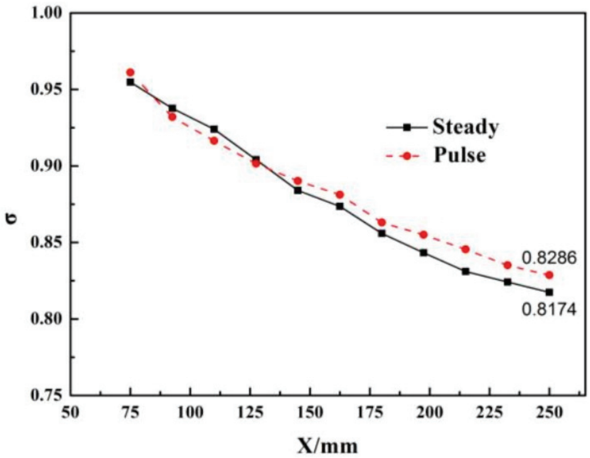

Figure 12 – Total pressure recovery coefficient downstream of X=75mm along the axial direction

Table 4 – Inner thrust of steady and pulse injection schemes

Scheme	Steady	Pulse
Inner thrust/kN	2.101	2.290
Difference	-	9.0%↑

4. Conclusions

Numerical results of high temperature transverse pulse injection supersonic combustion flow field are studied. Firstly, within the region of pulse interference, the flow field changes periodically. Secondly, the fuel mass flux of pulse jet is only a half of the steady jet in the pulse period, but the distribution of hydrogen and water is basically the same in the pulse interference zone, and the combustion surface is almost the same size. Thirdly, compared with the steady injection scheme, the amount of hydrogen combusted even 25.46% larger in the pulse interference zone, the total pressure recovery coefficient is 1.4% greater at the exit section of combustion chamber, and the inner thrust is 9.0% increased. Finally, the high temperature pulse injection scheme has a promoting effect on fuel mixing and combustion, which is as great as the combustion chamber performance in steady injection scheme while the fuel is saved.

References

[1] Pudsey A S, Boyce R R. Numerical Investigation of Transverse Jets Through Multiport Injector Arrays in Supersonic Crossflow[J]. Journal of Propulsion and Power, 2010, 26(6):1225-1236.

[2] Kummitha O R, Pandey K M, Gupta R. CFD analysis of a scramjet combustor with cavity based flame holders[J]. Acta Astronautica, 2018, 144:244-253.

[3] Dharavath M, Manna P, Chakraborty D. Numerical exploration of mixing and combustion in ethylene fueled scramjet combustor[J]. Acta Astronautica, 2015, 117: 305-318.

[4] Mishra D P, Sridhar K V. Numerical Study of Effect of Fuel Injection Angle on the Performance of a 2D Supersonic Cavity Combustor[J]. Journal of Aerospace Engineering, 2012, 25(2):161-167.

[5] Williams N J. Numerical Investigations of a High Frequency Pulsed Gaseous Fuel Jet Injection into a Supersonic Crossflow[D], University of Tennessee, 2016.

[6] Cutler A D, Harding G C, Diskin G S. High Frequency Pulsed Injection into a Supersonic Duct Flow[J]. AIAA Journal, 2013, 51(4): 809-818.

[7] Kouchi T, Sasaya K, Watanabe J, et al. Penetration Characteristics of Pulsed Injection into Supersonic Crossflow[C]// 46th AIAA/ASME/SAE/ASEE Joint Propulsion Conference & Exhibit, Nashville, 2013:1301-8.

[8] ZHOU Song-bai, Research on Numerical Method, Experimental Verification and Application in Simulating Jet Interaction in Supersonic External Flow[D]. Graduate School of National University of Defense Technology, 2009.

[9] FAN Xiao-feng, WANG Jiang-feng, ZHAO Fa-ming. Numerical Simulation of Multi-components Reacting Flow Using Roe Scheme[J]. Journal of Nanjing University of Aeronautics & Astronautics, 2016, 48(03):347-351.

[10]ZAHO Fa-ming. Numerical Investigation of High Temperature Non-equilibrium Flow and Multi-components RCS Jet Interaction[A]. China mechanics society hydromechanics Specialized Committee. Summary of the Ninth National Symposium on fluid mechanics, [C]. China mechanics society, fluid mechanics Specialized Committee, 2016:1.

[11]LIU Chen. Numerical Methods for Complex Combustion Flow Fields[D]. Nanjing University of Aeronautics and Astronautics, 2009.

[12]Baurle R, Mathur T, Gruber M, et al. A numerical and experimental investigation of a scramjet combustor for hypersonic missile applications[C]. AIAA/ASME//-SAE/ASEE Joint Propulsion Conference and Exhibit, 2013.

[13]Rust B. An Improved Lobed Strut Injector Concept for Supersonic Combustion[R]. AIAA, 2010-6962.

[14]TAN Jian-guo, WU Ji-ping, WANG Zhen-guo. Direct-connect experiment and numerical simulation on dual-combustor ramjet[J]. Journal of Aerospace Power, 2013,28(07): 1675-1680 Smith J, Jones B and Brown J. The title of the conference paper. *Proc Conference title*, where it took place, Vol. 1, paper number, pp 1-11, 2001.

Copyright Statement